Vol. 678: 109–124, 2021
https://doi.org/10.3354/meps13859

MARINE ECOLOGY PROGRESS SERIES
Mar Ecol Prog Ser

Published November 11[§]

# Stock structure and effective population size of the commercially exploited gummy shark *Mustelus antarcticus*

**Emma Petrolo[1,*], Jessica Boomer[1,2], Jessica O'Hare[1], Kerstin Bilgmann[3], Adam Stow[1]**

[1]Conservation Genetics Lab, Department of Biological Sciences, Macquarie University, Macquarie Park, NSW 2109, Australia
[2]Sydney Institute of Marine Science, 19 Chowder Bay Rd, Mosman, NSW 2088, Australia
[3]Marine Vertebrate Conservation and Evolution Lab, Department of Biological Sciences, Macquarie University, Macquarie Park, NSW 2109, Australia

ABSTRACT: The Australian gummy shark *Mustelus antarcticus* is distributed across southern and eastern Australian waters and is the main target of a large shark fishery. Commercial harvest of the species is considered sustainable based on biomass estimates that show recovery from past overexploitation. However, the effective population size and genetic-based assessments of stock structure remain unresolved. We evaluated the genetic structure and effective population size ($N_e$) of the gummy shark using genome-wide single nucleotide polymorphisms. We found genetic divergence between individuals from the east coast and those along the south coast, resulting in 2 discrete populations with signatures of adaptive divergence. Spatial analyses revealed widespread gene flow within each of these populations, with some evidence for mild isolation-by-distance observed using individual-based tests. Demographic modelling of each population showed a comparatively rapid decline of $N_e$ in the most recent past compared to more historical projections, with evidence that such declines have occurred to the point where genetic variation could be at risk. The identification of 2 divergent populations of gummy shark suggests that management should consider each individually to ensure the long-term sustainability of the species.

KEY WORDS: Gummy shark · Genetic structure · Effective size · Fisheries management



## 1. INTRODUCTION

Human exploitation has increasingly led to the global degradation of marine environments and a loss of biodiversity (Swartz et al. 2010, Hilborn & Ovando 2014, Ortuño Crespo & Dunn 2017). Currently, 24% of chondrichthyans (sharks and rays) are vulnerable to extinction due to overexploitation (Dulvy et al. 2014, Ortuño Crespo & Dunn 2017, Rubinas 2017). Commercial fisheries and the globalised trade of marine resources are considered the primary threats because they result in a reduction of recruitment and subsequent fishery production in exploited shark populations (Vasconcelos et al. 2014). Reductions in the size of isolated populations can result in a loss of genetic variation, increasing the risk of inbreeding depression and decreasing the potential of an evolutionary response to environmental change (Stow et al. 2001, Frankham et al. 2002, Frankham 2005, Mathur & DeWoody 2021). Consequently, describing genetic structure and loss of variation in harvested species contributes useful information towards sustainable management.

The genetic structure of commercially exploited species is often unknown or inferred from the spatial structuring of changes in catch biomass (Cadrin et al. 2013, Maunder & Piner 2015). Methodological developments enable many thousands of single nucleotide

*Corresponding author: emma.petrolo@hdr.mq.edu.au

[§]Corrections were made after publication. For details see www.int-res.com/articles/meps2021/679/m679p241.pdf
This corrected version: November 25, 2021

polymorphisms (SNPs) to be efficiently generated per individual, thereby providing opportunities for more frequent assessment of genetic structure. Facilitated by higher-resolution genetic markers, interest in genetic-based fisheries research has increased, with 127 research articles published on the topic between 1997–2016 (Benestan 2019). Describing genetic structure remains the most common aim because it allows for the delineation of significant management units — a principal management goal for commercially harvested species (Benestan 2019).

Population genetic approaches based on selectively neutral loci describe genetic structure that is primarily a consequence of gene flow and random genetic drift (Hare et al. 2011). The processes responsible for patterns of genetic connectivity can then be inferred by the association of gene flow with landscape features (Lowe & Allendorf 2010, Selkoe et al. 2016). Loci that are located within or physically linked to functional parts of the genome can be used to test for local adaptation (Momigliano et al. 2017). The selective processes involved are potentially revealed if there is sufficient information on the genome of the target species and its environmental parameters (Ahrens et al. 2018). Quantitative genetic approaches can also be applied; for example, fishing-induced selection was observed in Atlantic cod *Gadus morhua*, resulting in earlier maturation and smaller body size (Swain et al. 2007).

The rate at which genetic variation is lost and the influence of selection is a consequence of the effective population size ($N_e$). $N_e$ is the size of an ideal population that loses genetic variation at the same rate as the population being evaluated, with random genetic drift increasing as $N_e$ decreases and selection becoming more efficient as $N_e$ increases (Husemann et al. 2016). Multiple studies have shown that commercial harvest has the potential to reduce $N_e$ to the point where genetic variation is lost, even in populations of relatively large census sizes (Antao et al. 2011, Allendorf et al. 2014). Estimates of $N_e$ for commercially harvested species can be modelled to predict the future viability of populations (Hare et al. 2011).

The impacts of the global shark catch increase of the 1960s–1970s on genetic diversity and $N_e$ remain unknown for many harvested species (Swartz et al. 2010, Dulvy et al. 2014, Rubinas 2017). During this period, the commercial harvesting of sharks increased globally by 227% based on biomass catch estimates and continued to increase until peaking in 2003 and eventually declining by 15% before 2011 (Collie et al. 2016, Davidson et al. 2016). For example, persistent harvest of the school shark *Galeorhinus galeus* by the Australian southern shark fishery from the 1920s–1970s led to a drastic decline in their landings, and a subsequent switch in target species from the school shark to the more fecund gummy shark *Mustelus antarcticus* (Walker & Shotton 1999, Pribac et al. 2005, Walker et al. 2005). A rapid decline in gummy shark numbers followed between 1970 and 1997, where the species comprised 47% of the southern shark fishery catch (Walker & Shotton 1999). This resulted in a one-third reduction in their abundance (based on biomass catch estimates) along the south coast between 1973–1976 and 1998–2001 (Walker & Shotton 1999). Any impact on genetic variation caused by the population declines reported for gummy sharks has yet to be evaluated (Woodhams et al. 2018, Helidoniotis et al. 2019).

In order to estimate $N_e$, population genetic structure needs to be known, as $N_e$ is calculated for individual discrete genetic clusters (which will now be referred to as populations; Charlesworth 2009). The genetic structure of gummy sharks has remained inconclusive owing to conflicting evidence garnered from catch estimates and genetic studies (Ovenden et al. 2018). MacDonald (1988) utilised a single polymorphic allozyme locus as a marker for genetic variation throughout the southern coast of the species' range, finding no evidence for genetic structuring. Gardner & Ward (1998) expanded on this research, using 7 polymorphic allozyme loci to investigate potential genetic differentiation across the east and south coast, showing the presence of 2 separate populations. Samples indicated one population ranging from Newcastle to the Clarence River in New South Wales (NSW), and one ranging from Bunbury in Western Australia (WA) to Eden in lower NSW (Gardner & Ward 1998). Contrastingly, there was no evidence of genetic structure across the species' range using 8 microsatellite markers (Boomer & Stow 2010, Boomer 2013). Here, we used a more highly resolving SNP data set to ask (1) is there genetic partitioning across the distribution of *M. antarcticus*, (2) is there evidence of spatial or sex-based genetic partitioning, (3) has a genetic bottleneck occurred and (4) what is the effective population size?

## 2. MATERIALS AND METHODS

### 2.1. Sampling

All gummy shark tissue samples (n = 94) were sourced from commercial fishers operating in southern and eastern Australian waters (including Tasma-

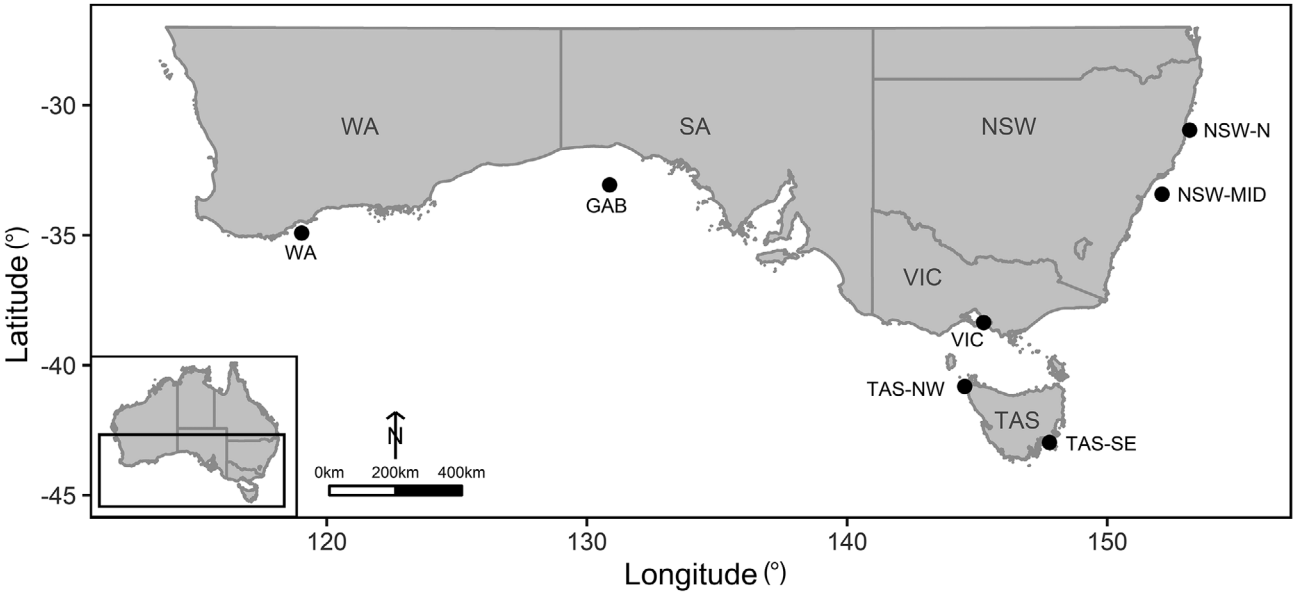


Fig. 1. Sites where gummy sharks *Mustelus antarcticus* were sampled within southern and eastern Australian waters (n = 7)

nia) from 2007–2010 (Boomer 2013). A ~1 $cm^3$ piece of muscle or fin tissue was collected from each sampled shark and stored in 70–90 % EtOH. The size and sex of each sampled shark was recorded, with all sharks sexed according to their external morphology. Age classes ranged from sub-adults to adults. Sample locations (n = 7) ranged from northern NSW to southern WA (Fig. 1, Table 1). Samples from 7 locations were included to assure good spatial coverage while maintaining sufficient statistical power at each location for subsequent analyses.

### 2.2. DNA extraction and sequencing

DNA extraction and sequencing was performed by Diversity Arrays Technology (DArT; www.diversityarrays.com). DNA was extracted from 0.5 $mm^3$ tissue sub-samples using the GeneCatch™ Blood and Tissue Genomic Mini Prep Kit (Epoch Life Science) following the manufacturer's guidelines. SNP discovery was performed for each sample using the standard DArTseq protocol (DArT 2018). DArTseq is a genotype-by-sequencing method (Sansaloni et al. 2011, Kilian et al. 2012) able to perform genome-wide marker discovery using the Illumina NGS platform (Andrews et al. 2016, Zhang et al. 2018). The DArTseq protocol is described in brief below.

As part of the DArTseq protocol and to ensure the quality of all genomic DNA, template DNA was incubated in a 1× solution of Multi-Core™ restriction enzyme buffer (Promega) for 2 h at 37°C. Approximately 100 ng $\mu l^{-1}$ of each DNA sample was then digested with a combination of the 2 restriction enzymes *Pst*I and *Sph*I. Each individual sample was ligated to unique barcodes and adapters specific to these enzymes. PCR amplification of each sample followed, using primers specific to the barcode and adaptor sequences. PCR conditions consisted of 1 min initial denaturation at 94°C, followed by 30 cycles of 20 s denaturation (94°C), 30 s annealing (58°C), 45 s extension (72°C) and a final extension of 7 min at 72°C. To prepare for hybridization to the flow cell, approximately 10 µl of each sample was pooled, diluted and denatured using NaOH. The subsequent library was sequenced on an Illumina HiSeq®2500 platform for 77 cycles, resulting in 77-bp-long frag-

Table 1. Sample sites and corresponding abbreviations (code), number of samples from each site and midpoint latitude and longitude estimates of their sampling location

| Site name | Code | n | Coordinates |
|---|---|---|---|
| NSW North Coast | NSW-N | 9 | 30° 57′ 39.4″ S, 153° 10′ 0.1″ E |
| NSW Mid Coast | NSW-MID | 17 | 33° 25′ 14.4″ S, 152° 6′ 25.7″ E |
| Western Port Bay, VIC | VIC | 10 | 38° 21′ 22.7″ S, 145° 14′ 52.8″ E |
| North-West Tasmania | TAS-NW | 15 | 40° 48′ 54.2″ S, 144° 31′ 11.1″ E |
| South-East Tasmania | TAS-SE | 13 | 42° 58′ 12.0″ S, 147° 46′ 48.0″ E |
| Great Australian Bight, SA | GAB | 15 | 33° 03′ 58.7″ S, 130° 52′ 12.2″ E |
| Albany, WA | WA | 15 | 34° 54′ 52.6″ S, 119° 2′ 19.3″ E |

ments (single read). A further 20% of the 94 samples were processed a second time following the preceding protocol to create a set of technical replicates that were used to later assess the reproducibility of SNP calls.

Individual samples were demultiplexed based on their unique ligated barcode. All remaining reads were checked for contamination using GenBank viral and bacterial example sequences alongside a database curated by DArT to ensure quality control of reads.

### 2.3. Generation of SNP data set

#### 2.3.1. Trimming sequences

Individual 'fastq' files were unzipped and relabelled, giving them unique IDs pertaining to their original sample source, with all replicates identified and labelled accordingly. Within each sequence, the prefix barcode was removed using the fastx-toolkit v.0.0.14 (Gordon & Hannon 2010), leaving the remaining *Pst*I restriction enzyme overhang. All barcodes were of random lengths, the maximum being 8 bp long. As a result, the shortest sequence was trimmed to 69 bp, with all remaining sequences trimmed to the same length to ensure comparability among reads (Gordon & Hannon 2010).

#### 2.3.2. Establishing parameters and filtering

Trimmed fastq files were processed de novo in the pipeline 'ipyrad' v.0.7.29 (Eaton & Overcast 2016). Ipyrad provides default parameters that detail the actions performed during the assembly of consensus sequences (Valencia et al. 2018). The assembly method follows 7 steps which assigns reads to individuals (1), filters for low-quality base calls (2), de novo clusters sequences (3) and estimates sequencing error rate and consensus allele sequences (4 & 5) before clustering consensus reads a final time (6) to output in variant call format (vcf) file (7). Where applicable, default parameters were modified to fit the specifications of the data set, with a preference for more stringent filtering options to create a high-quality SNP data set (see Supplement 1 at www.int-res.com/articles/suppl/m678p109_supp.pdf). VCFtools (Danecek et al. 2011) was used to filter and thin all identified SNP sites. Individuals with a read depth <40 000 were removed and replaced with a replicate sample of better quality where possible. Only polymorphic biallelic loci with <10% missing data, a minimum read depth >10 and a minor allele frequency (MAF) >0.05 were retained. The 2b-RAD perl script 'Hetfilter.pl' (Wang et al. 2012) was used to exclude sites with a heterozygosity >0.5 to guard against lumped paralogous loci. Additionally, the 2b-RAD perl script 'repMatchStats.pl' (Wang et al. 2012) was used to assess all technical replicates (n = 24 pairs) using the calculated heterozygosity discovery rate. Individuals that met the average heterozygosity were retained, and their replicate counterparts of lower quality were excluded from the final data set. Finally, the data set was thinned per 69 bp so that no 2 sites were within this specified distance of one another. The SNP data set and all following analysis scripts will be made available for public access in association with this paper.

#### 2.3.3. Identifying loci associated with selection

All remaining SNPs were further filtered to ensure a neutral data set. Hardy-Weinberg equilibrium (HWE) was calculated per individual locus using default Markov chain parameters in Genepop v.4.2 (Raymond & Rousset 1995, Rousset 2008). To account for Type I errors associated with multiple tests, all obtained p-values were converted to q-values using the package 'qvalue' v.2.16.0 (Dabney et al. 2004) in RStudio v.1.1.463 (R Core Team 2015). All loci that deviated from HWE at a false discovery rate of 5% ($q < 0.05$) were subsequently removed from the data set. Three $F_{ST}$ outlier tests were then implemented to identify SNPs carrying signals of selection. First, Arlequin v.3.0 (Excoffier et al. 2005) was run using all default parameters, applying a coalescent method which generates a null distribution of $F_{ST}$ using the island model of population structure (Excoffier et al. 2009). The p-values calculated by Arlequin were converted to q-values using the same method as previously mentioned. In addition, Bayescan v.2.1 (Foll & Gaggiotti 2008) was run using default parameters. Bayescan applies the Bayesian simulation method established by Beaumont & Balding (2004) to detect departures from neutrality between groups of loci. The subsequent output was visualised in R using a 5% false discovery rate (FDR) in the 'plot_bayescan' function. OutFLANK v.0.2 (Whitlock & Lotterhos 2015) was additionally run, with both the upper and lower 5% of inferred $F_{ST}$ distribution trimmed prior to estimation of the null model. All loci identified as outliers under a 5% FDR by any of the cited methods were subsequently removed from

the SNP data set. This method ensured greater confidence in the neutrality of the remaining SNP data set, thus the interpretation of their results.

All loci identified to be putatively under selection were run through the protein database search engine BLASTn (Altschul et al. 1990). Top results were identified based on a 90–100% identity match and an E-value of 1e-06.

### 2.4. Describing genetic differentiation and diversity

The R package 'adegenet' v.2.1.1 (Jombart & Ahmed 2011) was used to execute a *K*-means clustering analysis to identify the presence of distinct populations. These populations were then further explored in adegenet using the discriminant analysis of principal components (DAPC) function. This test was run 3 times to compare the influence of neutral vs. selective loci on genetic structure. Tests were based on all loci after HWE filtering, only loci identified to be putatively under selection and finally only neutral loci that remained in the data set after all filtering steps.

The residual data set of selectively neutral SNPs was used to evaluate genetic differentiation between sample sites in all subsequent analyses. Populations were then visualised using a principal components analysis (PCA; retaining 100 PCs) which employs the multivariate method designed by Jombart & Ahmed (2011). In addition, least-squares estimates of ancestry proportions (Frichot et al. 2014) were calculated using the R package LEA (Frichot & François 2015) to create a barplot of individual admixture coefficients based on the number of previously identified populations (*K*). Genetic differentiation was calculated as per Weir & Cockerham's (1984) method of estimating pairwise $F_{ST}$, using the 'diveRsity' v.1.9.90 (Keenan et al. 2013) package in R. Pairwise estimates were made based on 999 bootstraps with 95% bootstrapped CIs comparing each sampling location (n = 7) and each identified population.

Summary statistics were calculated to establish the genetic variation of each identified population. The R package 'strataG' (Archer et al. 2017) was used to calculate the number of private alleles ($N_p$), mean allelic richness ($A_r$), the proportion of polymorphic loci (PPL) and both the mean observed and expected heterozygosity ($H_o$, $H_e$) across all loci for each identified population. Wright's inbreeding coefficient ($F$) was calculated (per locus) based on the values of $H_o$ and $H_e$ determined by strataG.

### 2.5. Spatial analyses of genetic variation

Once populations were identified within the data set, spatial analyses of genetic variation were performed. Only populations that encompassed >2 sampling locations were included in the following spatial analyses.

Spatial autocorrelation analysis was performed in GenAlEx v.6.5 (Peakall & Smouse 2012) to explore genotypic similarity ($r$) between individuals on different spatial scales. Pairwise genetic (GD) and geographic distance (GGD) matrices were calculated for each analysis based on the input SNP and sample coordinate data, with all individuals collected from the same sampling location having the same coordinates (Table 1). Distance classes were chosen based on the maximum calculated GGD for each analysis, with distance classes chosen at even distances within the maximum threshold. Each spatial autocorrelation was run with 1000 bootstraps per distance class, generating (upper and lower) 95% CIs around each mean $r$. The null hypothesis (no spatial structure; $r = 0$) was tested using 999 permutations, generating (upper and lower) 95% CIs for each distance class. The presence of isolation-by-distance (IBD) was examined using heterogeneity tests (Banks & Peakall 2012). In addition, this data set was split between female (n = 41) and male (n = 29) individuals to explore the potential influence of sex on the spatial structure of $r$ for the species.

To further investigate the presence of IBD, the mixed-effects linear based maximum likelihood population effects model (MLPE) was run in R using the packages 'corMLPE' (Pope 2018) and 'nlme' (Pinheiro et al. 2012). The R package adegenet v.2.1.1 (Jombart & Ahmed 2011) was used to calculate Edward's genetic distance (Edwards 1971) between pairs of sites, which was then compared to the coordinate data of each site (Table 1) within the southern population (n = 70). Genetic distance and geographic distance (km) were compared using MLPE at the site level to explore the potential broad-scale spatial structuring of genetic diversity for the species. This analysis was used for both sexes combined due to sample size limitations at some locations when separating into males and females.

In addition, a Mantel test (Mantel 1967) was run in R using the package 'ade4' (Dray & Dufour 2007). A distance matrix was generated, mapping the Euclidean distance between the coordinates of each sample location. This matrix was then tested against the estimated genetic distance between corresponding sample locations. Calculations of genetic distance fol-

lowed the method described by Edwards (1971). Each analysis ran for 100 000 repetitions. Due to the recent conjecture surrounding the use of the Mantel method to test hypotheses of IBD (Harmon & Glor 2010, Legendre et al. 2015), the results of the preceding analyses are discussed in Supplement 1 (Fig. S1).

Finally, the R package 'SNPRelate' (Zheng et al. 2012) was used to calculate the within-site pairwise relatedness of all samples within the qualifying southern population (n = 70).

### 2.6. Estimating $N_e$ and the potential for bottleneck

The demographic history of *Mustelus antarcticus* was explored using the model-flexible method 'Stairway Plot', which estimates changes in $N_e$ based on site frequency spectra (SFS; Liu & Fu 2015). The model-flexible option is not restricted to a specific demographic model, subsequently exploring larger model space. Unique 'blueprint files' were created for each population as per the method outlined by Stairway Plot v.2 (Liu & Fu 2015). The blueprint files contained both default and unique parameters calculated specifically for the gummy shark, with all unique values obtained using the following methods. The pipeline 'easySFS' (Overcast 2017) was used to calculate the SFS of each identified population. SFS were calculated from the initial data set of raw variants identified in ipyrad (SNPs = 60 995), which preceded filtering for polymorphic biallelic loci and MAF (see Section 2.3.2). This was done since stringent filtering to exclude raw variants (particularly MAF) strongly affects calculations of SFS and can create a bias in the inference of population size (Linck & Battey 2019). As the specific mutation rate of the gummy shark is currently unknown, an estimate of mutation rate for the species was made based on the method followed by Galván-Tirado et al. (2013). In brief, a mutation rate of 0.62% per million years was used. This was calculated as the average of the known mutation rates for the scalloped hammerhead *Sphyrna lewini* (0.8%; Duncan et al. 2006), the sicklefin lemon shark *Negaprion acutidens* (0.67%; Schultz et al. 2008), the blacktip reef shark *Carcharhinus melanopterus* (0.43%; Keeney & Heist 2006) and the nurse shark *Ginglymostoma cirratum* (0.57%; Karl et al. 2012). Because Stairway Plots require mutation rates to be per generation, this average (0.62% per million years) was then divided by the generation time of *M. antarcticus* (16 yr; Woodhams et al. 2018) resulting in a mutation rate of 0.0000001. The total number of observed nucleic sites ($L$) was calculated based on the total number of loci (35 271) from the initial data set of identified raw variants (SNPs = 60995), multiplied by the number of base pairs (69; $L$ = 2 433 699).

## 3. RESULTS

### 3.1. Sample and SNP data set selection

Raw variants that were genotyped across all 94 individuals based solely on the initial input parameters selected for ipyrad contained 60 995 SNPs. Filtering of the raw data set in ipyrad for biallelic loci, MAF, heterozygosity and thinning for one site per read resulted in a data set of 9394 SNPs (Table 2). The greatest loss of SNPs during this process (48 950 SNPs removed) occurred during filtering for biallelic loci and a minimum MAF of 0.05 (Table 2).

A total of 137 loci significantly deviated from HWE ($q < 0.05$) and were removed, leaving 9257 SNPs (Table 2). Subsequent testing of this filtered data set (SNPs = 9257) for $F_{ST}$ outlier loci (FDR < 0.05) in Bayescan identified 214 loci under divergent selection, whilst Arlequin determined 60. All outlier loci previously identified in either Bayescan or Arlequin were also recognised by testing in OutFLANK, revealing 376 $F_{ST}$ outlier loci. As a result, all 376 loci recognised by OutFLANK were removed as being identified as putatively under positive selection by one or more $F_{ST}$ outlier tests (Table 2). Removal of these outliers resulted in a final neutral data set of 8881 SNPs which was used for all analyses unless indicated otherwise.

### 3.2. Genetic differentiation and diversity

A $K$-means clustering analysis inferred the presence of one population within the data set ($K$ = 1).

Table 2. Filtering steps undertaken following data assembly including number of single nucleotide polymorphisms (SNPs) retained for gummy shark populations in Australia. MAF: minor allele frequency; HWE: Hardy-Weinberg equilibrium

| Filtering step | No. of SNPs retained |
|---|---|
| Raw variants identified in ipyrad | 60 995 |
| Biallelic loci ≤ 0.1 missing; MAF ≥ 0.05 | 12 045 |
| Heterozygosity ≤ 0.5 | 11 995 |
| Thinning 69 (one site per read) | 9394 |
| HWE q ≥ 0.05 | 9257 |
| Putatively selectively neutral loci | 8881 |

However, *K*-scores pertaining to $K = 1$ (*K*-score = 654.0579) and $K = 2$ (*K*-score = 654.6453) were very similar. Further investigation through PCA analysis revealed a contrasting result—2 populations were identified in the data set (Fig. 2A). Amongst the identified populations, one population was found to encompass most individuals sampled from the east coast of Australia (east-pop, hereafter EP; n = 24), while the second population included the majority of the individuals sampled along the southern coast including Tasmania (south-pop, hereafter SP; n = 70). Two individuals sampled from the NSW-MID site (Fig. 1) were assigned to the inferred SP (Fig. 2A). Individuals within the EP were more densely grouped (Fig. 2A, axis 2) than those of the SP which were more broadly spread (Fig. 2A, axis 2), indicating individuals that are genetically similar to one another within populations, with less genetic variation within the EP when compared to the SP. These 2 populations

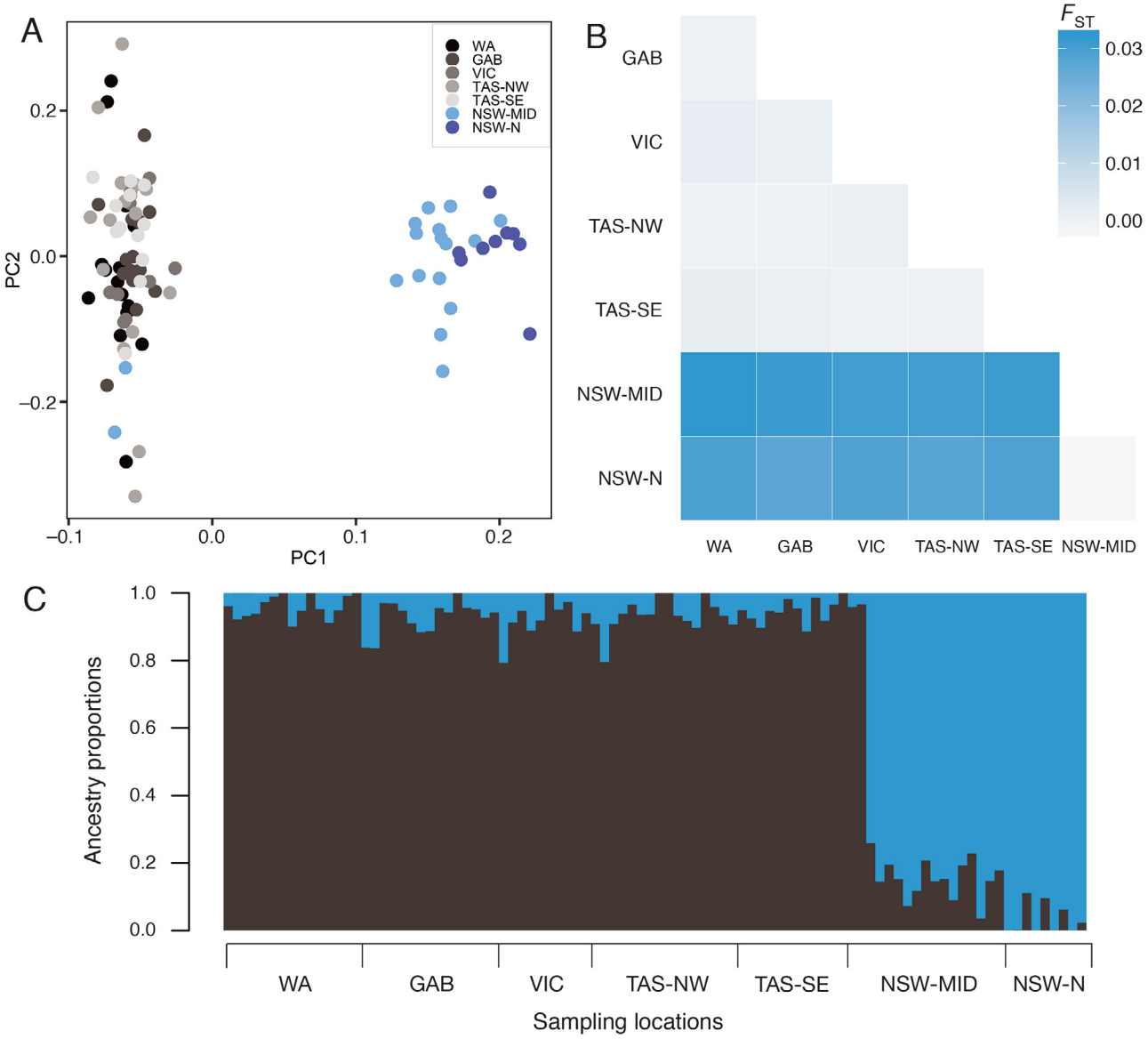


Fig. 2. (A) Principal component analysis (PCA) showing the separation of gummy shark individuals (n = 94; indicated by circle points) from 0 into 2 distinct groups. PCA of loci under positive selection (n = 376) returned comparable results (see Fig. S2). (B) Heat map displaying the variation of pairwise $F_{ST}$ values between each site ranging from −0.0001 to 0.0323. East-pop = NSW-N, NSW-MID; south-pop = TAS-NW, TAS-SE, WA, GAB, VIC (excluding the 2 individuals sampled from NSW); see Table 1 for site names. (C) Admixture plot displaying ancestry proportions of gene frequencies per individual (n = 94), with individuals assigned to populations ($K = 2$) based on shared co-ancestry. Each column denotes one individual. East-pop = blue; south-pop = black

were further supported by the admixture analysis when run with a $K$ of 2. Admixture proportions for each individual were minimal, with a strong gradient between blocks (Fig. 2C). Within the SP, 10 individuals were observed to share no ancestral alleles with the EP. Concurrently, within the EP, 5 individuals presented no admixture with the SP. The SP featured a maximum shared ancestry proportion admixed from the EP of 23%. Similarly, the maximum admixture of ancestral alleles from the SP to the EP was 22%. The 2 individuals sampled from the NSW-MID site that were genetically assigned to the SP had admixture proportions of 0.96 (SP) and 0.04 (EP), while all other individuals sampled within this group had average admixture proportions of 0.14 (SP) and 0.86 (EP). The genetic difference between the EP and SP was quantified in pairwise $F_{ST}$ calculations, which indicated moderate genetic difference between the EP and SP with the $F$-statistic of 0.0298 (95% CI: 0.0169–0.0447) being significantly different from zero. There is a clear distinction between the range of $F_{ST}$ values quantified between each population. Those comparing between-population sites are consistently higher (Fig. 2B; $F_{ST}$ = 0.0279–0.0323) than within-population site comparisons (Fig. 2B; $F_{ST}$ = –0.0001 to 0.007).

Summary statistics comparing both the EP and SP are presented in Table 3. There was a greater $N_p$ identified in the SP than in the EP (Table 3). Contrastingly, the mean $A_r$ was greater in the EP than in the SP (Table 3). PPL was comparably high for each population, ranging from 0.97–0.99 (EP to SP respectively; Table 3). Estimates of mean $H_o$ and $H_e$ indicate similar levels of genetic variation between each identified population (Table 3). Moreover, calculations of $F$ do not indicate a major deficit of heterozygosity within each population (Table 3).

Table 3. Number of private alleles ($N_p$), mean Allelic richness ($A_r$), proportion of polymorphic loci (PPL), mean observed heterozygosity ($H_o$), mean expected heterozygosity ($H_e$) and Wright's inbreeding coefficient ($F$) for gummy shark populations from the east coast (east-pop) and southern coast Australia including Tasmania (south-pop)

| | East-pop (n = 24) | South-pop (n = 70) |
|---|---|---|
| $N_p$ | 12 | 252 |
| $A_r$ | 0.0833 | 0.0294 |
| PPL | 0.97 | 0.99 |
| $H_o$ | 0.2374 | 0.2357 |
| $H_e$ | 0.2461 | 0.2468 |
| $F$ | 0.0351 | 0.0451 |

### 3.3. Loci associated with selection

Genetic divergence between the EP and SP was further strengthened when loci identified to be associated with selection were considered. Clustering analyses comparing the neutral data set (Fig. 3C) with a data set only including outlier loci (Fig. 3B) indicated that the signal of genetic structure was strongly influenced by loci associated with selection. Combining neutral and outlier loci into one data set concurrently revealed the presence of 2 distinct populations (Fig. 3A).

Conservative runs of BLASTn resulted in the match of 10 sequences to known genes (Table 4). The functions of each identified gene varied, with some having known physiological processes (e.g. limb morphogenesis), protein synthesis or immune system functioning (Table 4).

### 3.4. Spatial structure of genetic variation

Spatial analyses were performed on all individuals from the SP (n = 70) only, as the EP (n = 24) comprised 2 sampling locations. All spatial autocorrelation analyses of the SP (n = 70) included both individuals sampled from the east coast site (NSW-MID) that were identified as being genetically similar to the SP in analyses for genetic structure (Fig. 2A).

Analysis of all individuals in the SP identified positive spatial structure in the first distance category (within-site comparisons) and a significant decline in $r$ across the whole correlogram (heterogeneity test: omega = 68.584, $p < 0.01$). The calculated $r$-value was significantly greater than the null hypothesis at the 0 km distance class ($r = 0.014$, $p < 0.01$), with positive autocorrelation remaining until 348.419 km ($r$ = 0 intercept; Fig. 4A). Beyond the first distance class, there was little evidence of a decline in $r$ with geographic distance.

A decline in $r$ across the whole correlogram was identified by heterogeneity tests for both females (n = 41) and males (n = 29) in the SP (females: omega = 57.208, $p < 0.01$; males: omega = 41.139, $p < 0.01$). However, differences in the tested distance classes caused by the uneven sex ratio of samples at some sites (Table 5) means that calculations of $r$ are not directly comparable.

Both individuals sampled from the east coast site (NSW-MID) that were identified as genetically similar to the SP in analyses for genetic structure (Fig. 2A) were excluded from the MLPE and relatedness estimates, as the small sample size (n = 2) was not com-

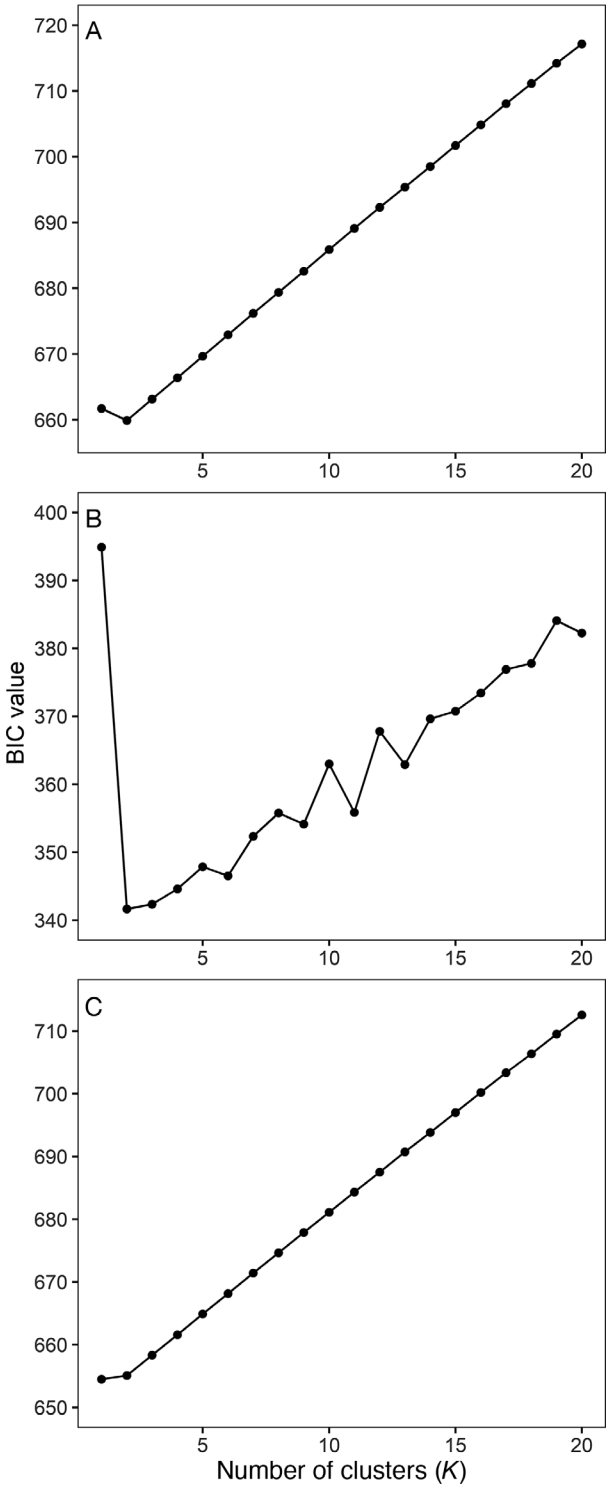


Fig. 3. Comparative plot identifying potential gummy shark populations for (A) all loci after Hardy-Weinberg equilibrium filtering (single nucleotide polymorphisms [SNPs] = 9257), (B) only loci identified to be putatively under selection (SNPs = 376) and (C) only neutral loci that remained in the data set after all filtering steps (SNPs = 8881). Potential number of populations ($K$) ranging from 0–20 with $K$ indicated by bayesian information criterion (BIC) value

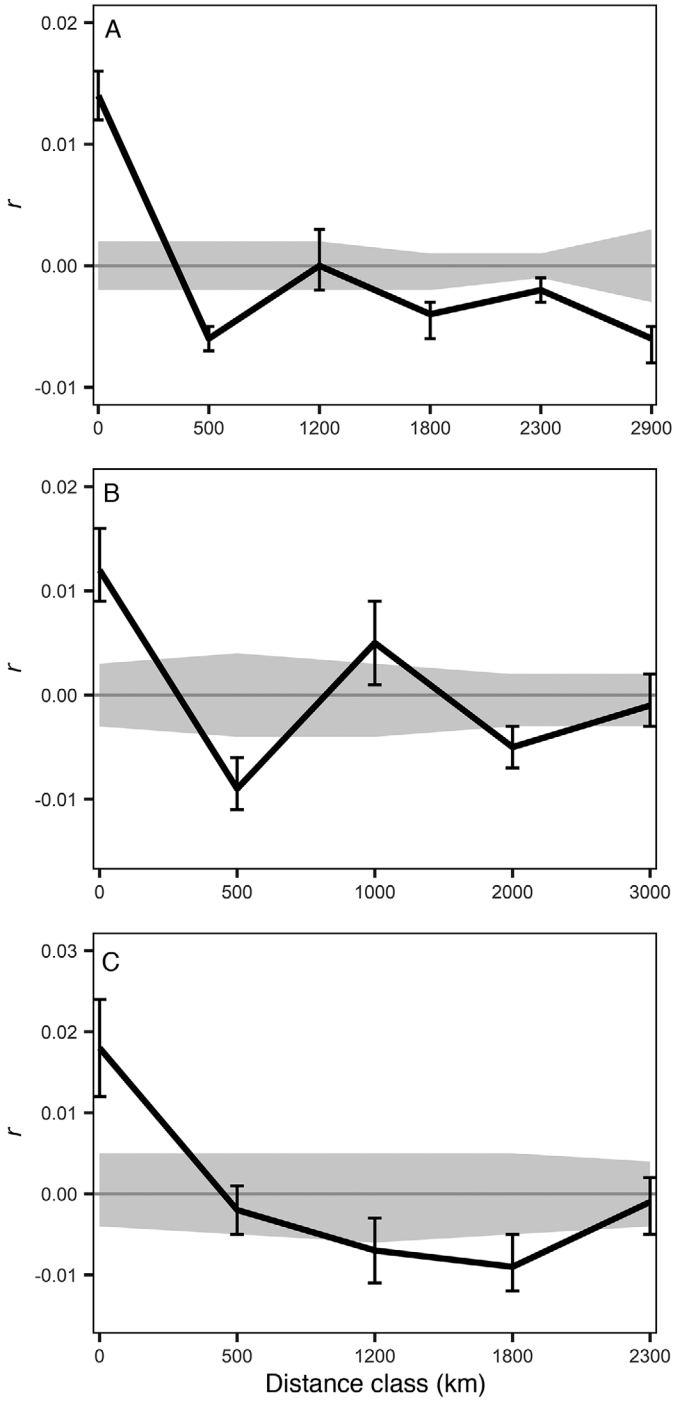


Fig. 4. Spatial correlogram comparing mean genotypic similarity ($r$) (A) within the south-pop across 6 different distance classes and between (B) female and (C) male gummy sharks. Distance classes in (A): 0 (n = 439), 500 (n = 345), 1200 (n = 375), 1800 (n = 431), 2300 (n = 600) and 2900 km (n = 195); (B): 0 (n = 136), 500 (n = 112), 1000 (n = 120), 2000 (n = 220) and 3000 km (n = 232); and (C): 0 (n = 79), 500 (n = 63), 1200 (n = 56), 1800 (n = 63) and 2300 km (n = 103). Solid black line: calculations of $r$ per distance class; black bars: 95% confidence intervals for each correlation value; grey line: null hypothesis; grey shading: 95% confidence intervals around the null hypothesis

Table 4. Annotated BLASTn results for $F_{ST}$ outlier loci (n = 376). SNP: single nucleotide polymorphism

| SNP | Top BLASTn hit | Accession no. | Ident/cov | E-value | Function (nil = unknown) |
|---|---|---|---|---|---|
| 9394 | Recombination activating gene 1 and 2 (*Carcharhinus plumbeus*) | AY172838.1 | 95/65 | 2e-13 | Both are multiprotein complexes that mediate the DNA cleavage phase during V(D)J recombination |
| 13961 | Mca234 microsatellite sequence (*Mustelus californicus* clone) | JF264895.1 | 92/98 | 1e-16 | Nil |
| 32167 | Cyclic phosphodiesterase 7A-like (LOC109937477; *Rhincodon typus*) | XM_020536057.1 | 90/62 | 9e-18 | Hydrolyses the second messenger cAMP to regulate some physiological processes. May have a role in muscle signal transduction |
| 66839 | Cluster_HOXD (*Scyliorhinus canicular*) | FQ032660.1 | 90/74 | 2e-12 | Essential determinant of limb morphogenesis |
| 86288 | Microsatellite Ape348 sequence (*Alopias pelagicus*) | MN719483.1 | 92/86 | 1e-09 | Nil |
| 97032 | T cell receptor gamma (*Carcharhinus plumbeus*) | FJ854492.2 | 92/68 | 5e-08 | Expression found predominantly in lymphoid and mucosal tissues, signifies TCR-expressing lymphocytes |
| 106787 | SA_Bc-114B5 (*Squalus acanthias* clone) | AC171389.4 | 90/32 | 2e-14 | Nil |
| 114619 | Uncharacterised LOC116981122 (*Amblyraja radiata*) | XR_004414169.1 | 95/31 | 1e-21 | Nil |
| 137675 | Lipoyl (octanoyl) transferase 2 (putative) (lipt2; *Rhincodon typus*) | XM_020531874.1 | 92/68 | 4e-09 | Protein involved in the first step of the subpathway that synthesizes protein N(6)-(lipoyl) lysine from octanoyl-[acyl-carrier-protein] |
| 157921 | MIP3 gene (*Triakis scylliu*) | AB174766.1 | 90/16 | 5e-15 | Immune response for macrophage inflammatory protein-3 alpha |

parable to the other sample sites included in the following population-level analyses (Fig. 5, Table 5).

No signal of IBD was identified by the MLPE analysis of the SP (Akaike information criterion, AIC = −68.118756, delta = 0, $p > 0.05$). A spatial pattern of genetic variation was not estimated, as there was no linear relationship between genetic and geographic distances within the SP (Fig. 5). The estimated genetic variation of individuals across the geographic range of samples was relatively homogenous, with genotypic distance decreasing by only 0.006 $D_{CSE}$ (Edward's distance) across the maximum 2500 km distance range. Comparisons of genetic distance were split between a higher genetic distance range (0.127–0.133 $D_{CSE}$) and a lower range (0.105–0.116 $D_{CSE}$) with no comparisons found outside these ranges. Comparison points within these upper and lower ranges are evenly spread across the sample sites, contributing to the geographic distance of the test (Fig. 5).

Table 5. Estimates of genotypic similarity per south-pop sample site, excluding the NSW-MID site south-pop associated samples (see Table 1 for site names). Gummy shark sex ratios (♀/♂), mean genotypic similarity (μ) and standard deviation (σ)

| Site name | ♀/♂ | μ | σ |
|---|---|---|---|
| GAB | 8/7 | 0.0007 | 0.0021 |
| TAS-NW | 8/7 | 0.0005 | 0.0023 |
| TAS-SE | 6/7 | 0.0008 | 0.0018 |
| WA | 9/6 | 0.0004 | 0.0012 |
| VIC | 8/2 | 0.0004 | 0.0010 |

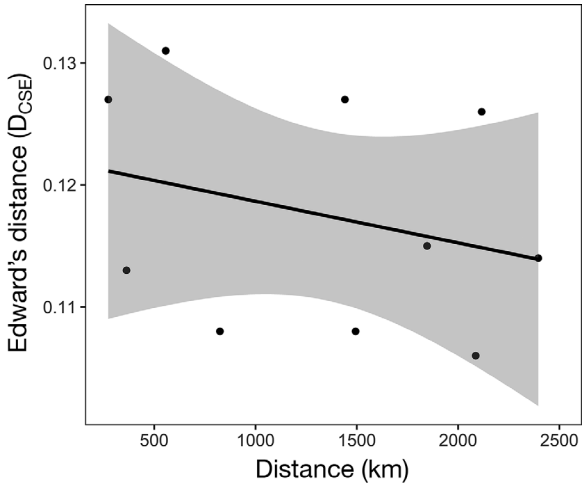


Fig. 5. Maximum likelihood population effects plot comparing the genotypic distance of all individuals in the south-pop (excluding the NSW-MID south-pop associated samples; n = 68) to the range of distances (km) encompassed by their associated sample sites. Dots: points of comparison (GenoDist/Dist) based on the number of individuals tested; shading: 95% CIs encompassing these comparisons

The average $r$ calculated for individuals within sample sites support a lack of significant IBD across the SP because estimates of $r$ between sites differed by a mean (μ) of only 0.0004 (Table 5). Estimates of within-site $r$ were generally consistent, inferring that elevated $r$ values present at the first distance class (0 km) for all spatial autocorrelations (Fig. 4) were not driven by a single location.

### 3.5. Estimates of $N_e$

Stairway Plot estimates showed temporal changes in $N_e$ for the EP and SP. Both populations followed a similar trend, where a gradual increase in $N_e$ from first calculations is followed by a long-standing plateau where both populations reached their highest estimated $N_e$ (Fig. 6, Tables S1 & S2 in Supplement 2). The first estimated decrease in $N_e$ for the EP occurred in the more recent past, with a gradual decline in size between 155 and 2 yr ago from 5400.424 to 1394.7342 individuals (Fig. 6B, Table S1). Within the SP, the first estimated decline occurred more recently and was comparably faster with a decrease in $N_e$ projections of 3188 individuals ($N_e$ of 783 predicted for the present day) occurring between 44 and 0.1128 yr ago (Fig. 6A, Table S2).

A range of CIs encompass these estimates, with the broadest intervals shown surrounding periods of gradual increase and decrease (Fig. 6, Tables S1 & S2). The particularly broad confidence intervals surrounding the gradual decreases observed for both populations in the most recent past as seen in Fig. 6 and Tables S1 & S2 will need to be considered in any interpretation of these results.

## 4. DISCUSSION

While marine ecosystems seemingly provide the right conditions for widespread dispersal and gene flow, species ranges are still often subdivided into distinct populations (Ovenden 2013, Puckett & Eggleston 2016). Our evidence of genetic partitioning into 2 gummy shark populations was well supported. One population included individual gummy sharks sampled from NSW sites north of Sydney (EP: NSW-N and NSW-MID; Fig. 1, Table1). Individuals sampled at all sites along the south coast (SP: VIC, TAS-NW, TAS-SE, GAB and WA; Fig. 1, Table 1) as well as 2 individuals sampled near Sydney, NSW, formed the second population. While gummy sharks seemingly have the capacity to disperse between the east and south coast of Australia, this occurrence must be rare, as ancestral gene frequencies show little admixture (Fig. 2C). In addition, there is some evidence that genetic divergence between these 2 populations may be a consequence of divergent selection (Table 4), suggesting that the 2 populations might represent evolutionarily significant units (ESUs; Crandall et al. 2000). The spatial structure of genetic variation within each of these

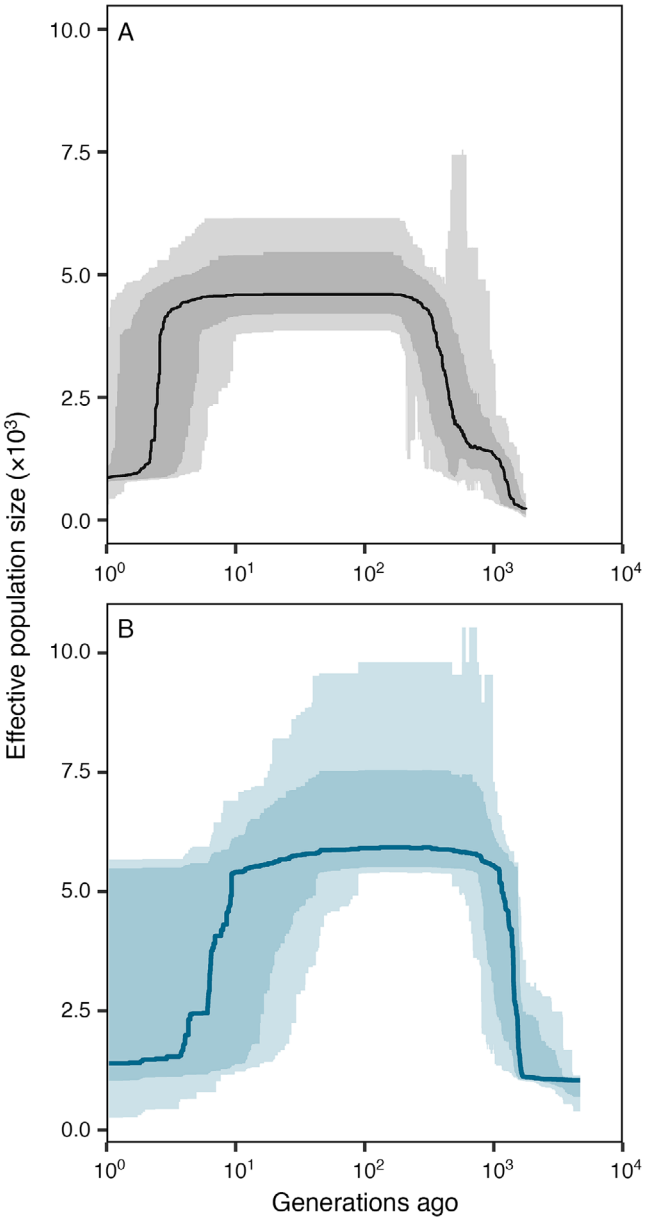


Fig. 6. Stairway Plot presenting estimated changes in effective population size ($N_e$) for the (A) south-pop from 28 447–0 yr ago, and (B) east-pop from 74 910–2 yr ago. Comparisons of changes in $N_e$ over time are made based on generation time (gummy shark = 16 yr); values presented are $\log_{10}$. Darker shading: 75% CIs; lighter shading: 95% CIs

populations suggests widespread gene flow, with some evidence for mild IBD observed in individual-based tests for the SP. Distinct populations form in response to a variety of biological and physical factors such as a species life history strategy, dispersal capacity, thermal tolerance and habitat requirements (Miller et al. 2013, Ovenden 2013).

Prevailing ocean currents can be associated with the development of genetic differentiation between regions, even in active-dispersing species that lack a pelagic larval stage (Mirams et al. 2011, Briggs & Bowen 2013). The East Australian Current (EAC) separates away from the continental shelf at ~33° S on the east coast, with only a remnant portion travelling southwards beyond this point (Ridgway 2007, Wijeratne et al. 2018). The more intense northern region of the EAC may discourage gummy shark dispersal to and from the SP, potentially as a consequence of shifts in resource availability (Ridgway 2007, Zeng et al. 2020). This would be particularly prevalent within the region of separation (~33° S), as this area is characterised by periodic eddy formation — presenting a potential barrier for both gummy sharks and their preferred food source of crustaceans and small teleosts (Ridgway 2007, Woodhams et al. 2018). The common dolphin *Delphinus delphis* is an example of an active-dispersing species seemingly influenced by this variation in oceanographic conditions, with genetic differentiation between groups located on either side of the area where the EAC separates (Möller et al. 2011, Barceló et al. 2021). Previous gummy shark research supports the pattern of genetic differentiation we resolved here. Two genetic groups were inferred using allozyme loci — one including individuals sampled from southern Australia to Eden on the east coast of NSW, and the other from Newcastle to the Clarence River in northern NSW (Gardner & Ward 1998).

Whilst an accurate boundary between the EP and SP cannot be confirmed by our study due to a lack of samples located in southern NSW, the presence of 2 individuals sampled from within NSW that were genetically assigned to the SP (Fig. 2A) indicates that our findings may be consistent with that of Gardner & Ward (1998). This hypothesis is particularly compelling, as these 2 individuals encompassed the southern-most portion of the NSW-MID site (~34° S), whilst the rest of the site samples were higher in latitude (above ~33° S). This split in population assignment may potentially be influenced by the region of separation of the EAC from the coast found at this latitude. The potential for the identified SP to extend to southern NSW is relevant to fisheries management, with further sampling in this region being required to resolve stock boundaries.

As a genus, *Mustelus* sharks generally display a high degree of sub-regional endemism largely consistent with biogeographic boundaries and fine-scale oceanographic processes (Maduna et al. 2020). Sandoval-Castillo & Beheregaray (2015) investigated the genetic structure of the commercially exploited brown smooth-hound *M. henlei* in the Gulf of California, observing significant genetic differentiation between individuals in neighbouring biogeographic regions, irrespective of their large dispersal capacity (~15 km daily). Recent acoustic monitoring of gummy shark mobility revealed that they are capable of long-distance displacements in the range of 238–900 km (Braccini et al. 2017). This large-scale dispersal potential is supported by the extent of admixture observed in within-population $F_{ST}$ results alongside spatial analyses, confirming that the species is adept at dispersing within the ranges of their respective SP or EP group with no sex-bias (Figs. 2B & 4).

Demographic modelling of both the EP and SP revealed fluctuations in $N_e$ over time (Fig. 6A,B). While each population exhibited a comparably rapid decline in $N_e$, they each had a unique genetic history whereby the projected timing and magnitude of these declines varied. Within the EP, the first estimated decrease in $N_e$ began ~200 yr ago and has continued to the present day (Fig. 6B). It can be assumed that a gradual decrease in census size contributed to this trend, as the key variable contributing to reductions in $N_e$ is population decline (Frankham 1995). This observation may have potentially resulted from an intensification of the EAC, with variation in the strength of the EAC estimated to have persisted for the past 300 yr (Thresher et al. 2004, Ridgway 2007). Shifts in the abundance and distribution of food resources and habitat availability are likely to have resulted from the temporal variability of the EAC, potentially leading to the observed decline in $N_e$ (van Putten et al. 2013, Woodhams et al. 2018).

A rapid decline in $N_e$ was estimated to have occurred as recently as ~50 yr ago within the SP, interrupting a long-standing plateau ~5000 yr long. During this decline, $N_e$ was observed to drop from 3970 to 841 individuals (10 yr ago; Fig. 6B, Table S2) and this corresponds to a time period where substantial population declines occurred from commercial harvest in this region (Walker & Shotton 1999). During this time period, an estimated one-third decrease in gummy shark catch along the south coast was observed by the Australian southern shark fishery

(recorded between 1973–1976 and 1998–2001), signalling widespread population loss across their targeted range (Walker & Shotton 1999). Whilst conclusions on the rate and timing of the observed decline in $N_e$ across each population should be interpreted as indicative given the broad confidence intervals (Fig. 6), they do suggest that population declines (irrespective of the cause) have occurred to the point where genetic variation could be at risk (Charlesworth 2009). This is supported by estimates of allelic richness, where lower genetic diversity within the SP is associated with a relatively large genetic bottleneck ($A_r$: EP = 0.0833, SP = 0.0294; Fig. 6, Table 3). Allelic richness can detect genetic drift on short time scales due to the sensitivity of this measure to the loss of rare alleles (Greenbaum et al. 2014, Pinsky & Palumbi 2014). A loss of genetic diversity will potentially limit the adaptive potential of the species to changing conditions (Kuparinen & Merilä 2007, Jorgensen et al. 2008).

Retaining an $N_e$ of approximately 1000 individuals is recommended to maintain evolutionary potential (Lynch & Lande 1998, Frankham et al. 2014). However, the impacts of regular population loss coupled with the overlapping generation times generally observed for marine fishes can result in losses of genetic diversity with $N_e < 3000$ (Pinsky & Palumbi 2014). Consequently, the present-day estimates of $N_e$ for the EP of 1394 individuals and the SP of 782 individuals could lead to future losses of genetic diversity. Increasing sample sizes would provide more precise estimates of $N_e$ and could also enable the use of newly developed genetic approaches to estimate population sizes, such as close-kin mark–recapture (Bravington et al. 2016).

Confirming that east and south coast individuals form separate genetic stocks endorses the view that each population should be managed separately. The genetic variation and structure of active-dispersers in east and southern Australian waters has received relatively little attention, with most information available on the influence of coastal currents and phylogeographic boundaries for marine invertebrates with a pelagic larval stage (Colgan 2015). Comparison of the genetic structure of gummy sharks to other co-distributed actively dispersing species with similar diets and broadly similar life-history traits, such as the commercially harvested dogfish complexes (*Deania* and *Centroscymnus* spp.), will help establish the generality of the EAC in generating genetic structure. Strengthening of the EAC has resulted in the waters of southeast Australia having a disproportionately large increase in temperatures (Johnson et al. 2011). In turn, this has been associated with changes in resource availability (Johnson et al. 2011). Knowledge of both the processes influencing connectivity and levels of genetic variation available for evolutionary responses contributes towards predicting the impact of these rapid environmental changes.

*Acknowledgements*. We acknowledge Australian commercial fishers for their assistance and support with sample collection. We are extremely grateful to Ken Graham and Will MacBeth (NSW Department of Primary Industries), Matias Braccini, Terry Walker and Lorenz Frick (Department of Primary Industries, DPI, Victoria) and Adam Barnett (University of Tasmania) for assistance with sample collection. We thank Wilbur Ashley, Natalie Hejl, Skye Davis, Sonu Yadav and Andrea Petrolo and 2 anonymous reviewers for their assistance with analyses and comments on an earlier version of the manuscript. This study was funded by Macquarie University through a staff and HDR grant.

## LITERATURE CITED

Ahrens CW, Rymer PD, Stow A, Bragg J, Dillon S, Umbers KD, Dudaniec RY (2018) The search for loci under selection: trends, biases and progress. Mol Ecol 27: 1342–1356

Allendorf FW, Berry O, Ryman N (2014) So long to genetic diversity, and thanks for all the fish. Mol Ecol 23:23–25

Altschul SF, Gish W, Miller W, Myers EW, Lipman DJ (1990) Basic local alignment search tool. J Mol Biol 215:403–410

Andrews KR, Good JM, Miller MR, Luikart G, Hohenlohe PA (2016) Harnessing the power of RADseq for ecological and evolutionary genomics. Nat Rev Genet 17:81–92

Antao T, Pérez-Figueroa A, Luikart G (2011) Early detection of population declines: high power of genetic monitoring using effective population size estimators. Evol Appl 4: 144–154

Archer FI, Adams PE, Schneiders BB (2017) stratag: an R package for manipulating, summarizing and analysing population genetic data. Mol Ecol Resour 17:5–11

Banks SC, Peakall R (2012) Genetic spatial autocorrelation can readily detect sex-biased dispersal. Molec Ecol 21:2092–2105

Barceló A, Sandoval-Castillo J, Stockin KA, Bilgmann K and others (2021) A matter of scale: population genomic structure and connectivity of fisheries at-risk common dolphins (*Delphinus delphis*) from Australasia. Front Mar Sci 8:616673

Beaumont MA, Balding DJ (2004) Identifying adaptive genetic divergence among 676 populations from genome scans. Molec Ecol 13:969–980

Benestan L (2019) Population genomics applied to fishery management and conservation. In: Oleksiak F, Rajora OP (eds) Population genomics: marine organisms. Springer, Cham, p 399–421

Boomer J (2013) Genetic panmixia for two commercially important sharks (*Mustelus antarcticus* and *M. lenticulatus*). PhD thesis, Macquarie University, Sydney

Boomer JJ, Stow AJ (2010) Rapid isolation of the first set of polymorphic microsatellite loci from the Australian gummy shark, *Mustelus antarcticus* and their utility

across divergent shark taxa. Conserv Genet Resour 2: 393–395
Braccini M, Rensing K, Langlois T, McAuley R (2017) Acoustic monitoring reveals the broad-scale movements of commercially important sharks. Mar Ecol Prog Ser 577:121–129
Bravington MV, Grewe PM, Davies CR (2016) Absolute abundance of southern bluefin tuna estimated by close-kin mark–recapture. Nat Commun 7:13162
Briggs JC, Bowen BW (2013) Marine shelf habitat: biogeography and evolution. J Biogeogr 40:1023–1035
Cadrin SX, Kerr LA, Mariani S (2013) Stock identification methods: applications in fishery science. Academic Press, London
Charlesworth B (2009) Effective population size and patterns of molecular evolution and variation. Nat Rev Genet 10:195–205
Colgan DJ (2015) Marine and estuarine phylogeography of the coasts of south-eastern Australia. Mar Freshw Res 67: 1597–1610
Collie JS, Botsford LW, Hastings A, Kaplan IC and others (2016) Ecosystem models for fisheries management: finding the sweet spot. Fish Fish 17:101–125
Crandall KA, Bininda-Emonds OR, Mace GM, Wayne RK (2000) Considering evolutionary processes in conservation biology. Trends Ecol Evol 15:290–295
Dabney A, Storey JD, Warnes G (2004) Q-value estimation for false discovery rate control. Medicine (Baltimore) 344:48
Danecek P, Auton A, Abecasis G, Albers CA and others (2011) The variant call format and VCFtools. Bioinformatics 27:2156–2158
DArT (Diversity Arrays Technology) (2018) DNA Extraction Protocol for DArT. https://ordering.diversityarrays.com/files/DArT_DNA_isolation.pdf (accessed 8 Nov 2018)
Davidson LN, Krawchuk MA, Dulvy NK (2016) Why have global shark and ray landings declined: Improved management or overfishing? Fish Fish 17:438–458
Dray S, Dufour AB (2007) The ade4 package: implementing the duality diagram for ecologists. J Stat Softw 22:1–20
Dulvy NK, Fowler SL, Musick JA, Cavanagh RD and others (2014) Extinction risk and conservation of the world's sharks and rays. eLife 3:e00590
Duncan KM, Martin AP, Bowen BW, De Couet HG (2006) Global phylogeography of the scalloped hammerhead shark (*Sphyrna lewini*). Mol Ecol 15:2239–2251
Eaton D, Overcast I (2016) ipyrad: interactive assembly and analysis of RADseq data sets. http://github.com/dereneaton/ipyrad
Edwards A (1971) Distances between populations on the basis of gene frequencies. Biometrics 27:873–881
Excoffier L, Laval G, Schneider S (2005) Arlequin (version 3.0): an integrated software package for population genetics data analysis. Evol Bioinform Online 1:47–50
Excoffier L, Hofer T, Foll M (2009) Detecting loci under selection in a hierarchically structured population. Heredity 103:285–289
Foll M, Gaggiotti O (2008) A genome-scan method to identify selected loci appropriate for both dominant and codominant markers: a Bayesian perspective. Genetics 180:977–993
Frankham R (1995) Effective population size/adult population size ratios in wildlife: a review. Genet Res 66:95–107
Frankham R (2005) Genetics and extinction. Biol Conserv 126:131–140
Frankham R, Briscoe DA, Ballou JD (2002) Introduction to conservation genetics. Cambridge University Press, Cambridge
Frankham R, Bradshaw CJ, Brook BW (2014) Genetics in conservation management: revised recommendations for the 50/500 rules, Red List criteria and population viability analyses. Biol Conserv 170:56–63
Frichot E, François O (2015) LEA: an R package for landscape and ecological association studies. Methods Ecol Evol 6:925–929
Frichot E, Mathieu F, Trouillon T, Bouchard G, François O (2014) Fast and efficient estimation of individual ancestry coefficients. Genetics 196:973–983
Galván-Tirado C, Díaz-Jaimes P, García-de León FJ, Galván-Magaña F, Uribe-Alcocer M (2013) Historical demography and genetic differentiation inferred from the mitochondrial DNA of the silky shark (*Carcharhinus falciformis*) in the Pacific Ocean. Fish Res 147:36–46
Gardner M, Ward R (1998) Population structure of the Australian gummy shark (*Mustelus antarcticus* Günther) inferred from allozymes, mitochondrial DNA and vertebrae counts. Mar Freshw Res 49:733–745
Gordon A, Hannon G (2010) Fastx-toolkit. FASTQ/A short-reads preprocessing tools. http://hannonlab.cshl.edu/fastx_toolkit/
Greenbaum G, Templeton AR, Zarmi Y, Bar-David S (2014) Allelic richness following population founding events–a stochastic modeling framework incorporating gene flow and genetic drift. PLOS ONE 9:e115203
Hare MP, Nunney L, Schwartz MK, Ruzzante DE and others (2011) Understanding and estimating effective population size for practical application in marine species management. Conserv Biol 25:438–449
Harmon LJ, Glor RE (2010) Poor statistical performance of the Mantel test in phylogenetic comparative analyses. Evolution 64:2173–2178
Helidoniotis F, Emery T, Woodhams J, Curtotti R (2019) Southern and eastern scalefish and shark fishery. In: Patterson H, Williams A, Woodhams J, Curtotti R (eds) Fishery status reports 2019. Australian Bureau of Agricultural and Resource Economics and Sciences, Canberra, p 114–131
Hilborn R, Ovando D (2014) Reflections on the success of traditional fisheries management. ICES J Mar Sci 71: 1040–1046
Husemann M, Zachos FE, Paxton RJ, Habel JC (2016) Effective population size in ecology and evolution. Heredity 117:191–192
Johnson CR, Banks SC, Barrett NS, Cazassus F and others (2011) Climate change cascades: shifts in oceanography, species' ranges and subtidal marine community dynamics in eastern Tasmania. J Exp Mar Biol Ecol 400:17–32
Jombart T, Ahmed I (2011) adegenet 1.3-1: new tools for the analysis of genome-wide SNP data. Bioinformatics 27: 3070–3071
Jorgensen C, Enberg K, Dunlop E, Arlinghaus R and others (2008) The role of fisheries-induced evolution — response. Science 320:48–50
Karl SA, Castro AL, Garla RC (2012) Population genetics of the nurse shark (*Ginglymostoma cirratum*) in the western Atlantic. Mar Biol 159:489–498
Keenan K, McGinnity P, Cross T, Crozier W, Prodöhl P (2013) diveRsity: an R package for the estimation of population genetics parameters and their associated errors. Methods Ecol Evol 4:782–788

Keeney DB, Heist EJ (2006) Worldwide phylogeography of the blacktip shark (*Carcharhinus limbatus*) inferred from mitochondrial DNA reveals isolation of western Atlantic populations coupled with recent Pacific dispersal. Mol Ecol 15:3669–3679

Kilian A, Wenzl P, Huttner E, Carling J and others (2012) Diversity arrays technology: a generic genome profiling technology on open platforms. In: Pompanon F, Bonin A (eds) Data production and analysis in population genomics. Methods in molecular biology, Vol 888. Humana Press, Totowa, NJ, p 67–89

Kuparinen A, Merilä J (2007) Detecting and managing fisheries-induced evolution. Trends Ecol Evol 22:652–659

Legendre P, Fortin MJ, Borcard D (2015) Should the Mantel test be used in spatial analysis? Methods Ecol Evol 6: 1239–1247

Linck E, Battey C (2019) Minor allele frequency thresholds strongly affect population structure inference with genomic data sets. Mol Ecol Resour 19:639–647

Liu X, Fu YX (2015) Exploring population size changes using SNP frequency spectra. Nat Genet 47:555–559

Lowe WH, Allendorf FW (2010) What can genetics tell us about population connectivity? Mol Ecol 19:3038–3051

Lynch M, Lande R (1998) The critical effective size for a genetically secure population. Anim Conserv 1:70–72

MacDonald CM (1988) Genetic variation, breeding structure and taxonomic status of the gummy shark *Mustelus antarcticus* in southern Australian waters. Mar Freshw Res 39:641–648

Maduna SN, Hull KL, Farrell ED, Boomer JJ and others (2020) Historical biogeography of smoothhound sharks (genus *Mustelus*) of Southern Africa reveals multiple dispersal events from the Northern Hemisphere. Syst Biodivers 18:633–645

Mantel N (1967) The detection of disease clustering and a generalized regression approach. Cancer Res 27:209–220

Mathur S, DeWoody JA (2021) Genetic load has potential in large populations but is realized in small inbred populations. Evol Appl 14:1540–1557

Maunder MN, Piner KR (2015) Contemporary fisheries stock assessment: many issues still remain. ICES J Mar Sci 72: 7–18

Miller AD, Versace VL, Matthews TG, Montgomery S, Bowie KC (2013) Ocean currents influence the genetic structure of an intertidal mollusc in southeastern Australia — implications for predicting the movement of passive dispersers across a marine biogeographic barrier. Ecol Evol 3:1248–1261

Mirams A, Treml EA, Shields J, Liggins L, Riginos C (2011) Vicariance and dispersal across an intermittent barrier: population genetic structure of marine animals across the Torres Strait land bridge. Coral Reefs 30:937–949

Möller L, Valdez FP, Allen S, Bilgmann K, Corrigan S, Beheregaray LB (2011) Fine-scale genetic structure in short-beaked common dolphins (*Delphinus delphis*) along the East Australian Current. Mar Biol 158:113–126

Momigliano P, Harcourt R, Robbins W, Jaiteh J, Mahardika GN, Sembiring A, Stow A (2017) Genetic connectivity and signatures of selection in grey reef sharks (*Carcharinus amblyrhychos*). Heredity 119:142–153

Ortuño Crespo G, Dunn DC (2017) A review of the impacts of fisheries on open-ocean ecosystems. ICES J Mar Sci 74:2283–2297

Ovenden JR (2013) Crinkles in connectivity: combining genetics and other types of biological data to estimate movement and interbreeding between populations. Mar Freshw Res 64:201–207

Ovenden JR, Dudgeon C, Feutry P, Feldheim K, Maes GE (2018) Genetics and genomics for fundamental and applied research on elasmobranchs. In: Carrier JC, Heithaus MR, Simpfendorfer CA (eds) Shark research: emerging technologies and applications for the field and laboratory. CRC Press, Boca Raton, FL, p 235–254

Overcast I (2017) easySFS. GitHub, https://github.com/isaacovercast/easySFS

Peakall R, Smouse PE (2012) GenAlEx 6.5: genetic analysis in Excel. Population genetic software for teaching and research — an update. Bioinformatics 28:2537–2539

Pinheiro J, Bates D, DebRoy S, Sarkar D (2012) nlme: linear and nonlinear mixed effects models. R package version 3

Pinsky ML, Palumbi SR (2014) Meta-analysis reveals lower genetic diversity in overfished populations. Mol Ecol 23: 29–39

Pope N (2018) CorMLPE: a correlation structure for symmetric relational data. GitHub, https://github.com/nspope/corMLPE/commit/80100fcf02c86a85431e72bf61df9368da822772

Pribac F, Punt AE, Walker T, Taylor B (2005) Using length, age and tagging data in a stock assessment of a length selective fishery for gummy shark (*Mustelus antarcticus*). J Northwest Atl Fish Sci 35:267–290

Puckett B, Eggleston D (2016) Metapopulation dynamics guide marine reserve design: importance of connectivity, demographics, and stock enhancement. Ecosphere 7: e01322

R Core Team (2015) R: a language and environment for statistical computing. Version 3.2.0. R Foundation for Statistical Computing, Vienna. https://www.R-project.org/

Raymond M, Rousset F (1995) GENEPOP (version 1.2): population genetics software for exact tests and ecumenicism. Heredity 86:248–249

Ridgway KR (2007) Long-term trend and decadal variability of the southward penetration of the East Australian Current. Geophys Res Lett 34:L13613

Rousset F (2008) Genepop'007: a complete reimplementation of the Genepop software for Windows and Linux. Mol Ecol Resources 8:103–106

Rubinas M (2017) Using knowledge of shark biology and behavior to inform management and conservation efforts for the globally distributed and fishery exploited shortfin mako (*Isurus oxyrinchus*). MSc thesis, Nova Southeastern University, Fort Lauderdale, FL

Sandoval-Castillo J, Beheregaray LB (2015) Metapopulation structure informs conservation management in a heavily exploited coastal shark (*Mustelus henlei*). Mar Ecol Prog Ser 533:191–203

Sansaloni C, Petroli C, Jaccoud D, Carling J, Detering F, Grattapaglia D, Kilian A (2011) Diversity Arrays Technology (DArT) and next-generation sequencing combined: genome-wide, high throughput, highly informative genotyping for molecular breeding of Eucalyptus. BMC Proceedings 5(Suppl 7):P54

Schultz JK, Feldheim KA, Gruber SH, Ashley MV, McGovern TM, Bowen BW (2008) Global phylogeography and seascape genetics of the lemon sharks (genus *Negaprion*). Mol Ecol 17:5336–5348

Selkoe KA, Aloia CC, Crandall ED, Iacchei M and others (2016) A decade of seascape genetics: contributions to basic and applied marine connectivity. Mar Ecol Prog Ser 554:1–19

Stow AJ, Sunnucks P, Briscoe D, Gardner M (2001) The impact of habitat fragmentation on dispersal of Cunningham's skink (*Egernia cunninghami*): evidence from allelic and genotypic analyses of microsatellites. Mol Ecol 10:867–878

Swain DP, Sinclair AF, Hanson JM (2007) Evolutionary response to size-selective mortality in an exploited fish population. Proc R Soc B 274:1015–1022

Swartz W, Sala E, Tracey S, Watson R, Pauly D (2010) The spatial expansion and ecological footprint of fisheries (1950 to present). PLOS ONE 5:e15143

Thresher R, Rintoul SR, Koslow JA, Weidman C, Adkins J, Proctor C (2004) Oceanic evidence of climate change in southern Australia over the last three centuries. Geophys Res Lett 31:L07212

Valencia LM, Martins A, Ortiz EM, Di Fiore A (2018) A RAD-sequencing approach to genome-wide marker discovery, genotyping, and phylogenetic inference in a diverse radiation of primates. PLOS ONE 13:e0201254

van Putten IE, Jennings S, Frusher S, Gardner C and others (2013) Building blocks of economic resilience to climate change: a south east Australian fisheries example. Reg Environ Change 13:1313–1323

Vasconcelos RP, Eggleston DB, Le Pape O, Tulp I (2014) Patterns and processes of habitat-specific demographic variability in exploited marine species. ICES J Mar Sci 71:638–647

Walker T, Shotton R (1999) Southern Australian shark fishery management. In: Shotton R (ed) Case studies of the management of elasmobranch fisheries. FAO, Rome, p 480–514

Walker TI, Hudson RJ, Gason AS (2005) Catch evaluation of target, by-product and by-catch species taken by gillnets and longlines in the shark fishery of south-eastern Australia. J Northw Atl Fish Sci 35:505–530

Wang S, Meyer E, McKay JK, Matz MV (2012) 2b-RAD: a simple and flexible method for genome-wide genotyping. Nat Methods 9:808–810

Weir BS, Cockerham CC (1984) Estimating *F*-statistics for the analysis of population structure. Evolution 38:1358–1370

Whitlock MC, Lotterhos KE (2015) Reliable detection of loci responsible for local adaptation: inference of a null model through trimming the distribution of $F_{ST}$. Am Nat 186:S24–S36

Wijeratne S, Pattiaratchi C, Proctor R (2018) Estimates of surface and subsurface boundary current transport around Australia. J Geophys Res Oceans 123:3444–3466

Woodhams J, Green C, Lyle J, Braccini M, Rogers P, Peddemors V (2018) Gummy shark (2018). http://fish.gov.au/report/181-Gummy-Shark-2018 (accessed 11 Mar 2019)

Zeng C, Rowden AA, Clark MR, Gardner JP (2020) Species-specific genetic variation in response to deep-sea environmental variation amongst Vulnerable Marine Ecosystem indicator taxa. Sci Rep 10:2844

Zhang L, Yang X, Qi X, Guo C, Jing Z (2018) Characterizing the transcriptome and microsatellite markers for almond (*Amygdalus communis* L.) using the Illumina sequencing platform. Hereditas 155:14

Zheng X, Levine D, Shen J, Gogarten SM, Laurie C, Weir BS (2012) A high-performance computing toolset for relatedness and principal component analysis of SNP data. Bioinformatics 28:3326–3328

*Editorial responsibility: Alistair Hobday, Hobart, Tasmania, Australia*
*Reviewed by: A. Lowther, P. Feutry*

*Submitted: January 20, 2021*
*Accepted: August 6, 2021*
*Proofs received from author(s): October 25, 2021*